Allostatic-interoceptive anticipation of social rejection

Joaquín Migeot , Eugenia Hesse , Sol Fittipaldi , Jhonny Mejía , Matías Fraile , Adolfo M. García , María del Carmen García , Rodrigo Ortega , Brian Lawlor , Vladimir Lopez , Agustín Ibáñez

PII: S1053-8119(23)00351-8
DOI: https://doi.org/10.1016/j.neuroimage.2023.120200
Reference: YNIMG 120200

To appear in: *NeuroImage*

Received date: 31 March 2023
Revised date: 11 May 2023
Accepted date: 26 May 2023

Please cite this article as: Joaquín Migeot , Eugenia Hesse , Sol Fittipaldi , Jhonny Mejía , Matías Fraile , Adolfo M. García , María del Carmen García , Rodrigo Ortega , Brian Lawlor , Vladimir Lopez , Agustín Ibáñez , Allostatic-interoceptive anticipation of social rejection, *NeuroImage* (2023), doi: https://doi.org/10.1016/j.neuroimage.2023.120200

Highlights

- Anticipatory interoceptive signals increase during unexpected social rejection.
- Negative HEP modulations reflect larger interoceptive signals in uncertainty.
- Key brain allostatic-interoceptive network hubs found via intracranial recordings.
- Exteroceptive signals are modulated by anticipation of reward-related outcomes.
- Findings inform models of allostatic interoception in social stress.

Allostatic-interoceptive anticipation of social rejection

Anticipation of social rejection

Joaquín Migeot[#1,2], Eugenia Hesse[#3,4], Sol Fittipaldi[1,3,5], Jhonny Mejía[1], Matías Fraile[3] Adolfo M. García[3,5,6], María del Carmen García[7], Rodrigo Ortega[1], Brian Lawlor[5], Vladimir Lopez[8]*, Agustín Ibáñez[1,3,4,5,9]*

[1] Latin American Brain Health Institute (BrainLat), Universidad Adolfo Ibáñez, Santiago, Chile

[2] Center for Social and Cognitive Neuroscience (CSCN), School of Psychology, Universidad Adolfo Ibanez, Santiago, Chile

[3] Cognitive Neuroscience Center (CNC), Universidad de San Andrés, Buenos Aires, Argentina

[4] National Scientific and Technical Research Council (CONICET), Buenos Aires, Argentina

[5] Global Brain Health Institute, University of California, San Francisco, United States and Trinity College Dublin, Ireland

[6] Departamento de Lingüística y Literatura, Facultad de Humanidades, Universidad de Santiago de Chile, Santiago, Chile

[7] Hospital Italaiano, Buenos Aires, Argentina

[8] Pontificia Universidad Catolica de Chile, Chile

[9] Predictive Brain Health Modelling Group, Trinity College Dublin (TCD), Dublin, Ireland

First authors

* Corresponding authors: Vladimir Lopez (vlopezh@uc.cl) and Agustin Ibanez (agustin.ibanez@gbhi.org)

Declarations of interest: none

Acknowledgments

AI is partially supported by grants ANID/FONDECYT Regular (1210195 and 1210176 and 1220995); ANID/FONDAP/15150012; ANID/PIA/ANILLOS ACT210096;

ANID/FONDEF ID20I10152 and ID22I10029; ANID/FONDAP 15150012; Takeda CW2680521 and the MULTI-PARTNER CONSORTIUM TO EXPAND DEMENTIA RESEARCH IN LATIN AMERICA [ReDLat, supported by National Institutes of Health, National Institutes of Aging (R01 AG057234), Alzheimer's Association (SG-20-725707), Rainwater Charitable foundation – Tau Consortium, and Global Brain Health Institute)]. Adolfo García is an Atlantic Fellow at the Global Brain Health Institute (GBHI) and is supported with funding from GBHI, Alzheimer's Association, and Alzheimer's Society (Alzheimer's Association GBHI ALZ UK-22-865742); ANID (FONDECYT Regular 1210176); and Programa Interdisciplinario de Investigación Experimental en Comunicación y Cognición (PIIECC), Facultad de Humanidades, USACH. Vladimir Lopez is partially supported by grants ANID/FONDECYT Regular (1210195). The contents of this publication are solely the responsibility of the authors and do not represent the official views of these Institutions.

Abstract

Anticipating social stress evokes strong reactions in the organism, including interoceptive modulations. However, evidence for this claim comes from behavioral studies, often with inconsistent results, and relates almost solely to the reactive and recovery phase of social stress exposure. Here, we adopted an allostatic-interoceptive predictive coding framework to study interoceptive and exteroceptive anticipatory brain responses using a social rejection task. We analyzed the heart-evoked potential (HEP) and task-related oscillatory activity of 58 adolescents via scalp EEG, and 385 human intracranial recordings of three patients with intractable epilepsy. We found that anticipatory interoceptive signals increased in the face of unexpected social outcomes, reflected in larger negative HEP modulations. Such signals emerged from key brain allostatic-interoceptive network hubs, as shown by intracranial recordings. Exteroceptive signals were characterized by early activity between 1-15 Hz across conditions, and modulated by the probabilistic anticipation of reward-related outcomes, observed over distributed brain regions. Our findings suggest that the anticipation of a social outcome is characterized by allostatic-interoceptive modulations that prepare the organism for possible rejection. These results inform our understanding of interoceptive processing and constrain neurobiological models of social stress.

Introduction

Social rejection is a form of social stress that constitutes one of the most primal painful experiences, eliciting bodily responses comparable to those of physical damage (Chae et al., 2022; Eisenberger, 2012, 2015). Social interactions are critical during adolescence and lay the groundwork for later social functioning (Blakemore and Mills, 2014; Orben et al., 2020). Positive social interactions protect against mental health problems and promote

brain health and resilience, but they become risk factors for the development of affective disorders in the presence of bullying, loneliness, and/or social rejection (Orben et al., 2020), promoting abnormal brain maturation (Raufelder et al., 2021; Tyborowska et al., 2018) and adult psychopathology (Laceulle et al., 2019). The anticipation of a social outcome (acceptance or rejection) has been related to interoception (i.e., sensing or perceiving signals about physiological body states (Tsakiris and Critchley, 2016)), as accurate sensing of somatic signals can guide cognition and socioemotional behavior to face rejection (e.g., when an invitation to a date is expected to be declined, accurate information about the current state of the organism is needed to exercise efficient self-regulation, so as not to under/overreact to the response to the invitation) (Durlik et al., 2014; Wu et al., 2021), with relevant mechanisms being further modulated by the frequency of previous favorable outcomes (Billeke et al., 2015; Billeke et al., 2020; Billeke et al., 2014). Nevertheless, evidence on this phenomenon comes from behavioral studies limited to the counting of heartbeats during the anticipation of public speaking (Durlik et al., 2014; Stevens et al., 2011; Wu et al., 2021), often with inconsistent results. For instance, Durlik et al. (2014) showed that participants evidenced increased interoceptive accuracy during speech anticipation, while Stevens et al. (2011) reported that both low and high anxiety groups did not. To address these issues, here we proposed an allostatic-interoceptive approach (Kleckner et al., 2017; Migeot et al., 2022) to assess brain correlates of social outcomes anticipation.

Allostatic-interoceptive predictive coding frameworks propose that the brain integrates organismic and environmental signals to anticipate possible scenarios and generate adaptive responses (Nord and Garfinkel, 2022; Petzschner et al., 2021; Quigley et al., 2021; Schulkin and Sterling, 2019; Sterling, 2014). Specifically, this process is indexed by the allostatic interoceptive network, a large-scale brain network that modulates visceromotor and interoceptive processes multimodally, including regions such as the anterior cingulate, insular, and prefrontal cortex (Kleckner et al., 2017). The anticipation triggered by interoceptive (Durlik et al., 2014; Wu et al., 2021) and exteroceptive (Peters et al., 2017) information during social outcomes might be adaptive; for instance, seeking a new social group after being rejected by another. Social rejection modulates interoception (Durlik et al., 2014; Durlik and Tsakiris, 2015; Stevens et al., 2011; Wu et al., 2021) and increases allostatic load (i.e., progressive wear and tear in the body from chronic exposures to environmental stressors, demanding repetitive energy relocation processes to attend those demands) (Larrabee Sonderlund et al., 2019). Critically, a combined allostatic-interoceptive approach to the anticipation of social rejection would help to characterize the interoceptive and exteroceptive processes involved in social rejection.

Here, we develop an interoceptive and exteroceptive approach to brain anticipatory responses (Vanhollebeke et al., 2022) using a social rejection task. We assessed the heart-evoked potential (HEP), an EEG measure of interoception elicited by cardiac signals and regulated by the ability to feel the body (Coll et al., 2021). Also, the HEP indexes allostatic

processing associated with anticipation and coping with uncertainty, operationalized in terms of prediction inferences (i.e., expected activity) and prediction errors (i.e., degree of mismatch between the prediction of expected activity over the actual activity) (Birba et al., 2022; Migeot et al., 2022; Tumati et al., 2021). Then, we evaluated the exteroceptive underlying oscillatory activity in the relevant alpha (Hofmann, 2006; Hofmann et al., 2005) and delta (Poppelaars et al., 2018; Poppelaars et al., 2021) bands. Despite the body of EEG research on social rejection, commonly employing tasks aimed at inducing social stress by receiving likability judgments (for a meta-analysis, see Vanhollebeke et al. (2022)), no study has investigated its interoceptive and exteroceptive anticipatory processes.

An adapted version of a social rejection task (Somerville et al., 2006) allowed us to compare cardiac and stimulus-related changes (HEP and oscillatory modulations, respectively) during the anticipation of the response when inviting someone to join a social network. Also, intracranial EEG recordings (iEEG) allowed us to further examine its spatiotemporal correlates with the best resolution available, overcoming the limitation of other neuroimaging techniques (Chennu et al., 2013; Hesse, 2022; Hesse et al., 2016a; Mikulan et al., 2018b) and providing a unique characterization of the neural basis of the anticipation of social rejection. Concerning interoceptive signals, we hypothesized that the larger the uncertainty about the social outcome, the greater the allostatic processing, reflected in larger HEP modulations (Birba et al., 2022; Legaz et al., 2022; Tumati et al., 2021). Also, based on the neurocognitive organismic preparatory process evoked under uncertainty (Peters et al., 2017), we expect interoceptive signals to arise from key allostatic interoceptive network regions (e.g., insula and anterior cingulate cortex) (Kleckner et al., 2017). As regards exteroceptive signals, we hypothesize that the larger the uncertainty about the social outcome, the greater the oscillatory power in low-frequency bands (Hofmann, 2006; Hofmann et al., 2005; Poppelaars et al., 2018; Vanhollebeke et al., 2022) from relevant frontotemporal regions (e.g., prefrontal cortex, precuneus, and anterior cingulate cortex) (Rappaport and Barch, 2020). By employing EEG measures accompanied by spatiotemporal neuroanatomical correlates with better signal-to-noise ratio (iEEG), this approach may illuminate the brain dynamics of the anticipatory phase of social rejection.

Materials and Methods

Participants

We recruited 58 adolescents as part of a larger ongoing protocol. All of them volunteered and assented following parental authorization and informed consent. One participant was discarded due to poor signal-to-noise ratio in his EEG recordings, resulting in a final sample of 57 (31 female) participants between the ages of 8 and 18 (12.96 ± 3.52). Normal cognitive functioning was verified in each participant through two psychological assessment sessions and interviews with their tutors. This was followed by the social

rejection task, performed while EEG and electrocardiographic (ECG) signals were recorded. The study was approved by the local institutional review board and performed in accordance with the Declaration of Helsinki.

The study also included three patients with intractable epilepsy who were offered surgical intervention to alleviate their condition. They were all part of an ongoing iEEG protocol (Birba et al., 2017; Garcia-Cordero et al., 2017; Garcia et al., 2020; Hesse et al., 2016b; Hesse et al., 2019; Mikulan et al., 2018a). Subject one was a 29-year-old male, subject two was a 32-year-old male, and subject three was a 49-year-old female. They had been suffering from drug-resistant epilepsy since they were 16, 10, and 14 years old, respectively, and none of them had a history of drug or alcohol abuse. All of them were implanted with 385 depth electrodes and monitored 24 hours a day, for seven days. During this time, each participant completed an adapted version of the experimental task used in the EEG study. Patients 2 and 3 also underwent ECG recordings while they performed the task, enabling assessment of the intracranial HEP (iHEP) (Garcia-Cordero et al., 2017; Park et al., 2018). All subjects gave written informed consent in accordance with the Declaration of Helsinki, and the study was approved by the local institutional review board.

Experimental design

The social rejection task was designed and executed on Presentation® software (Version 18.0, Neurobehavioral Systems, Inc., Berkley, CA, www.neurobs.com). It consisted of an initial setup phase followed by the actual task. Instructions were provided orally and then recapped on screen.

Stimuli comprised portraits of students who did not attend the participants' schools. Photos were shot at the students' schools with a Panasonic AG-HMC40P digital camera, 150 cm from the face, against a white background. As in the original design of the social rejection task (Somerville et al., 2006), participants were also photographed (though their photos were not included as stimuli) and led to believe that students from other schools would be forming impressions of them. Participants chose the photo they liked most and would upload to a social network. The luminosity and contrast of the photos were treated to gain uniformity. After an initial screening, three sets of 120 photos were obtained pertaining to age groups 8-10, 12-14, and 16-18 years old. A validation was then conducted with an independent preliminary sample composed of 30 participants, 10 from each age group. These subjects were asked to rank each person's likeability and propensity to be invited into a social network, on a scale from 1 to 7. After visual inspection of the photos and descriptive analysis of the responses, three final sets (100 per age group) were obtained excluding photos of poor technical quality or those that attained ≥ 10% of potential invitations.

During the setup phase, subjects were presented with 100 pictures of age-appropriate faces (50% female). They were instructed to select 50 of those pictures as if they were people that would invite to be part of their social network. According to the monitor size, around 20 faces were presented simultaneously and organized in five pages. Arrows at the left and right sides of the screen allowed the subject to navigate back and forth between the pages of pictures. A counter of how many "people" the subject had selected was displayed on the top of the screen. When the subject had selected 50 faces, the setup phase ended, and the task started.

Each trial of the task (**Figure 1**) began with a blank screen (1000 ms), followed by a fixation cross (200 ms). Stimulus onset occurred after a random time interval (between 300 and 500 ms). A picture of one of the 100 faces presented during setup was shown along with an indication of whether the participant had invited that person to his/her social network (green check) or not (red cross). The subject then guessed whether their invite would be accepted or not by pressing pre-assigned keyboard buttons. After 2000 ms, feedback on their guess (i.e., actual acceptance or rejection of the invite) was presented during 1000 ms. To assure a sufficient number of trials per condition each picture was presented twice, resulting in a total number of 200 trials presented in two blocks of 100 trials each.

The social rejection task allows to measure the anticipatory, reactive and recovery phases of social stress exposure (Vanhollebeke et al., 2022). Here, to focus on our aims (i.e., anticipation) and avoid excessive complexity in the statistical design, we analyzed the anticipatory phase only. The task comprises four conditions during this phase (**Figure 1**). First, Acceptance/Rejection trials are based on the guessed response, meaning that the participant anticipates an acceptance or rejection of the invite, respectively. Second, Compatible/Incompatible trials are determined by the coincidence or discrepancy between the choice and guessed response, respectively, based on the level of uncertainty on the assumption of reciprocity of the invite (i.e., anticipating to receive the same outcome reported in the choice phase, thus, expecting to be accepted by those invited and rejected by those who were not). Third, Rejection-guessed trials are further subdivided into Compatible and Incompatible trials. Finally, Acceptance-guessed trials are subdivided into Compatible and Incompatible trials. Because by design the task trial types were dynamically generated according to the participants' guess to induce uncertainty by manipulating the incidence of Acceptance and Rejection trials, we assessed the equivalence of trial type count per condition (**Figure 1**, **Supplementary material 1**). Additionally, we measured heart-rate variability (HRV) to control for potential cardiac artifacts when comparing among conditions (**Figure 1**, **Supplementary material 2**).

INSERT FIGURE 1 HERE

Figure 1. **Social Rejection Task**. *Left*: Sequence of screens presented during a single trial with their associated display duration. The time interval between Guess and Feedback corresponds to the anticipatory phase. *Upper Right*: Trial count percentages. Contrasts between conditions revealed that Acceptance trials were more frequently presented to subjects during the task, and within these, Compatible ones were more frequent; whereas Rejection trials presented a higher frequency for Incompatible ones (**Supplementary material 1**). *Lower Right*: heart rate variability (ms) for each condition. Contrasts between conditions did not show significant differences between either of them (**Supplementary material 2**). ***p* < .001, * *p* < .05; HRV: heart rate variability; SOA: stimulus onset asynchrony.

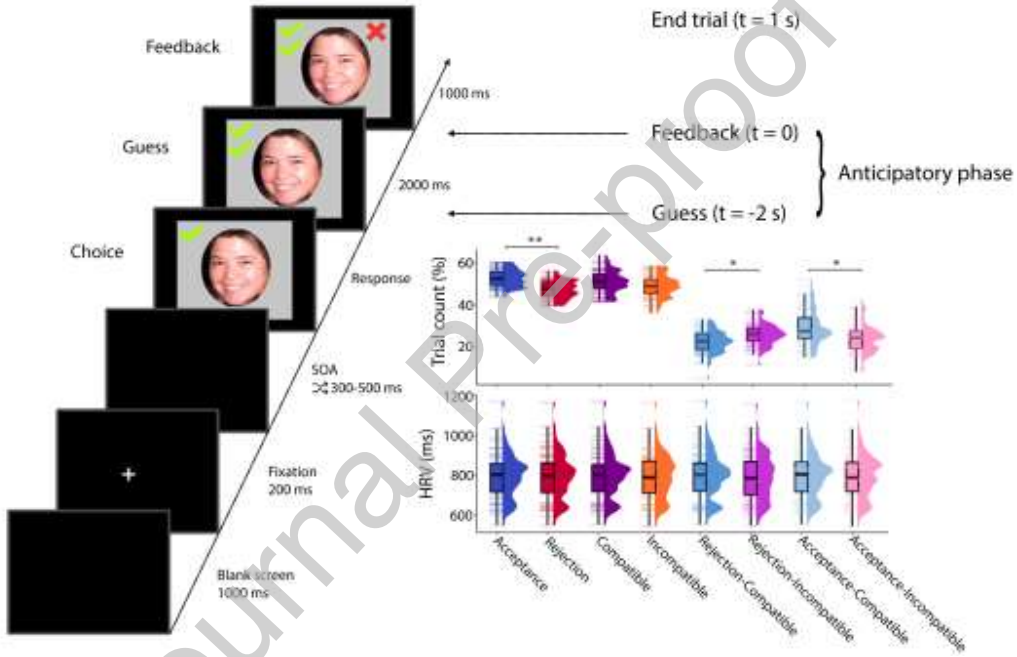

Statistical analysis

EEG

Signal preprocessing

EEG were acquired using a Biosemi 64 + 8 system (Biosemi, Amsterdam, the Netherlands) at a 2048 Hz sampling rate. Electrodes were placed in a cap according to the 10/20 system. The reference was set to mastoids during acquisition, and then it was re-referenced offline to the average of all electrodes. Signals were down-sampled offline to 512 Hz and band-pass filtered from 0.1 Hz to 40 Hz. Signals acquired during the setup phase were discarded. Channels with poor signal-to-noise ratio were visually identified and subsequently interpolated using spherical interpolation. Then, eye movements, blinks, and heart artifacts

were corrected with independent component analysis (Kim and Kim, 2012). All EEG preprocessing steps were performed on Matlab (Higham and Higham, 2016) using custom scripts and EEGLab (Delorme and Makeig, 2004).

HEP

To analyze HEP-related modulations during the task, preprocessed EEG signals were segmented in epochs locked to the R peak, with a temporal duration that included 200 ms prior to the R waveform onset to 800 ms after (Birba et al., 2022; Couto et al., 2014; Legaz et al., 2020), within the Anticipatory phase (2000 ms pre-feedback). This time window (-200 to 800) was utilized based on prior studies to circumvent two sources of confounding factors: the cardiac artifact occurring within the 0-200 ms range and the potential contamination from subsequent heartbeats in later windows (>800 ms) (Kern et al., 2013; Park et al., 2014). Trials that were more than 2.5 standard deviations away from the mean probability distribution were discarded, and the remaining ones were, once again, visually inspected to remove those with poor signal-to-noise ratio (Salamone et al., 2020). Finally, they were baseline corrected considering the time interval from -200 ms to 0 ms and grand averaged for each subject and condition separately.

Because HEP is a negative deflection mainly reflected in central and frontal electrodes around 200-600 ms post R waveform onset (peak) (Garcia-Cordero et al., 2016; Muller et al., 2015; Pollatos et al., 2016; Pollatos and Schandry, 2004), we assessed modulations in frontocentral electrodes (26 electrodes: Fp1, AF7, AF3, F7, F5, F3, FT7, FC5, FC3, Fpz, AFz, F1, Fz, F2, FC1, FCz, FC2, Fp2, AF4, AF8, F4, F6, F8, FC4, FC6, FT8) in this time interval. Moreover, subsets within this pool of electrodes were examined to obtain more specific insights into left (9 electrodes: Fp1, AF7, AF3, F7, F5, F3, FT7, FC5, FC3), central (8 electrodes: Fpz, AFz, F1, Fz, F2, FC1, FCz, FC2), and right (9 electrodes: Fp2, AF4, AF8, F4, F6, F8, FC4, FC6, FT8) regions of interest (ROI) (Couto et al., 2015; Garcia-Cordero et al., 2016; Yoris et al., 2018; Yoris et al., 2017). Statistical comparisons were performed to compare different conditions via point-by-point Monte Carlo permutation tests (5000) with bootstrapping (Rosenblad, 2009) and False Discovery Rate (FDR)-corrected in every ROI. Significantly different consecutive time points between conditions (Acceptance vs Rejection, Compatible vs Incompatible, Rejection-Compatible vs Rejection-Incompatible, Acceptance-Compatible vs Acceptance-Incompatible) were considered as such ($p < .05$) if sustained differences (30 ms) were present. In addition, topoplots of the mean difference between conditions in HEP modulation during the time interval considered (200-600 ms) were obtained for each ROI.

Oscillations

Anticipatory oscillatory activity in different conditions were derived from time-frequency charts. First, artifact-free preprocessed signals were segmented in epochs spanning 2500 ms pre-feedback per trial. Then, time-frequency charts were computed using the newtimef.m function from EEGLab (Delorme and Makeig, 2004) employing Fourier Fast Transform with Hanning tapers, a window size of 500 ms, window-centered, and a step of 9 ms (overlap of 99.1%). The charts were baseline corrected by subtracting the mean baseline oscillatory activity from -2500 ms to -2000 ms pre-feedback (that is, 500 ms before the guess). Statistical analyses were performed through Monte Carlo permutation tests (2000) with bootstrapping (Rosenblad, 2009) and FDR correction to test for significant modulations against baseline ($p < .05$). This procedure was performed for every condition (Acceptance, Rejection, Compatible, Incompatible, Rejection-Compatible, Rejection-Incompatible, Acceptance-Compatible, Acceptance-Incompatible), and for the same ROIs included in HEP analyses previously described. Topoplots reflecting the difference in oscillatory activity between conditions were obtained to account for the spatial domain.

We performed additional analyses considering the oscillatory activity in the frequency range of 1-15 Hz given that it has been implicated in social rejection dynamics (Hofmann, 2006; Hofmann et al., 2005; Poppelaars et al., 2018), as corroborated by our time-frequency charts. First, for every ROI, we averaged the oscillatory modulation between 1 and 15 Hz and performed statistical comparisons using point-by-point Monte Carlo permutation tests (5000 permutations) with FDR correction to examine differences ($p < .05$ sustained for 150 ms) between the conditions of interest (Acceptance vs Rejection, Compatible vs Incompatible, Rejection-Compatible vs Rejection-Incompatible, Acceptance-Compatible vs Acceptance-Incompatible). Then, we examined time-frequency clusters using FieldTrip (Oostenveld et al., 2011). Time-frequency charts were averaged in both time (from -2000 ms to 0 ms) and frequency (1 - 15 Hz). Cluster-based Monte Carlo permutation tests (2000 permutations) were performed between conditions including all recorded electrodes. A channel's activity was considered significant if it had at least two neighboring channels, as estimated by radial distance, with statistically significant modulations ($p < .05$). Significant channels were identified in the time-frequency topoplots.

iEEG

Signal acquisition and preprocessing

IEEG signals were acquired through a video-SEEG monitoring system (Micromed) with semi-rigid, multi-lead electrodes implanted in each patient. The electrodes (DIXI Medical Instruments) had a diameter of 0.8 mm and consisted of 5, 10, or 15 2 mm wide contact leads, interspaced by 1.5 mm within each electrode. Overall, 383 contact sites were available across subjects (126, 145, and 113 sites for Subjects 1, 2, and 3, respectively). The recordings were sampled at 512 Hz. ECG recordings were registered only in Subjects 2

and 3 through two adhesive electrodes placed in lead-II positions. Post-implantation MRI and CT scans were obtained for each patient. These were affine registered and normalized using a standardized protocol (Stolk et al., 2018) based on the FieldTrip (Oostenveld et al., 2011) toolbox that runs under Matlab (Higham and Higham, 2016). Montreal Neurological Institute (MNI) coordinates of each contact site were obtained from the MRIcron software (Rorden and Brett, 2000), and their corresponding brain region was located using the cuizuFindStructure function found in the SPM12 toolbox (http://www.fil.ion.ucl.ac.uk/spm/) (Ashburner and Friston, 1997). We used the normalized location of the electrode contact sites to an MNI coordinate space to examine the patients' results in a common space (Foster et al., 2015; Parvizi and Kastner, 2018) and were visualized through BrainNet Viewer (Xia et al., 2013) toolbox (downloaded from www.nitrc.org), that runs under Matlab (Higham and Higham, 2016).

Data were bandpass filtered between 0.1 Hz to 200 Hz and a Notch filter at 50 Hz and its harmonic frequencies (100 Hz and 150 Hz) was applied using EEGLab's (Delorme and Makeig, 2004) default settings. Then, channels were discarded if one or more of the following conditions were met: they exhibited pathological or artefactual waveforms under visual inspection; signal values did not exceed five times the signal mean; consecutive signal samples did not exceed five standard deviations (*SD*) from the gradient's mean; contact sites were located in white matter or epileptogenic zones as identified by expert epilepsy neurologists (MCG, JCA, WS) (Foster et al., 2015; Garcia et al., 2020; Hesse et al., 2016b; Hesse et al., 2019; Parvizi and Kastner, 2018). The remaining channels were referenced to the mean to further remove noise within the recordings. After signal preprocessing, 103, 92, and 70 electrodes remained in Subject 1, Subject 2, and Subject 3, respectively.

iHEP

Subjects 2 and 3 partook in iHEP analyses because ECG recordings were unavailable for Subject 1. Epochs were obtained following the same steps applied to EEG signals, except that all electrodes were explored individually. R-wave onset peaks were identified and signals were segmented into epochs (-200 ms to 800 ms relative to onset) and baseline corrected. The iHEP (Garcia-Cordero et al., 2017) does not follow the negative polarity inversion observed in the HEP (i.e., the greater the interoceptive modulation, the larger the negative voltage), as the sources represent different dipoles with non-homogenous distributions.

Statistical comparisons between conditions were made via point-by-point Monte Carlo permutation tests (5000 permutations) with bootstrapping (Rosenblad, 2009) and FDR correction in every electrode from Subjects 2 and 3. Significantly different consecutive time points between conditions (Acceptance vs Rejection, Compatible vs Incompatible,

Rejection-Compatible vs Rejection-Incompatible, Acceptance-Compatible vs Acceptance-Incompatible) were considered as such ($p < .05$) if sustained differences (30 ms) were present in the same direction throughout the epoch. Results were plotted in circular graphs using the package Circlize (Gu et al., 2014) that runs in R software (R Core Team, 2021).

Oscillations

To study anticipatory iEEG oscillatory activity, preprocessed signals were segmented into epochs (2500 ms pre-feedback). Then, electrodes were grouped by region within each subject and the averaged epochs were transformed into the time-frequency domain, following the same steps described for the EEG signals. From the resulting time-frequency charts, several frequency ranges were considered: delta (1-4 Hz), theta (4-8 Hz), alpha (8-13 Hz), beta (13-30 Hz), gamma (30-80 Hz), and high-frequency oscillations (80-120 Hz). Within these ranges, time-frequency signals were averaged and statistical comparisons were performed using point-by-point Monte Carlo permutation tests (5000 permutations) with FDR correction to examine differences ($p < .05$ sustained for 150 ms in the same direction throughout the epoch) between the conditions of interest (Acceptance vs Rejection, Compatible vs Incompatible, Rejection-Compatible vs Rejection-Incompatible, Acceptance-Compatible vs Acceptance-Incompatible). Results were plotted in circular graphs using the package Circlize (Gu et al., 2014) that runs in R software (R Core Team, 2021).

Results

EEG: Interoceptive signals were modulated by unexpected anticipations

First, when contrasting Acceptance vs Rejection trials, no differences were found in HEP considering frontal electrodes (5000 permutations, bootstrapping, FDR, $p < .05$) (**Figure 2**, first row).

Second, relative to Compatible trials, Incompatible ones showed larger negative HEP modulations around 350 ms to 550 ms in left frontal electrodes (5000 permutations, bootstrapping, FDR, $p < .05$) (**Figure 2**, second row).

Lastly, Rejection-Incompatible trials yielded larger negative HEP modulations than Rejection-Compatible trials in left frontal electrodes around 350 to 500 ms (5000 permutations, bootstrapping, FDR, $p < .05$) after Guess (**Figure 2**, third row).

As expected, interoceptive anticipation was modulated by the degree of predictability but not acceptance. These effects were null for anticipation within Acceptance trials.

EEG: Oscillatory power was modulated by anticipation in early, low-frequency bands

Time-frequency charts revealed early activity in the low-frequency band of 1-15 Hz, during approximately the first 400 ms after Guess for Acceptance and Rejection conditions relative to baseline (2000 permutations, bootstrapping, FDR, $p < .05$) at frontal electrodes. Averages in that frequency range showed significant differences (2000 permutations, bootstrapping, FDR, $p < .05$) between conditions, with greater event-related spectral perturbation (ERSP) during Acceptance trials. In addition, mean time-frequency topoplots for the subtraction between conditions showed differences in frontal and central electrodes, as reflected by significantly clustered electrodes (2000 permutations, $p < .05$) (**Figure 2**, first row).

As for the Acceptance and Rejection trials, time-frequency charts presented an early low frequency-activity at 1-15 Hz after Guess for Compatible and Incompatible conditions relative to baseline (2000 permutations, bootstrapping, FDR, $p < .05$) at left frontal electrodes. However, averages in that frequency range failed to present significant differences (2000 permutations, bootstrapping, FDR, $p < .05$) between conditions. Similarly, no significant clusters were found (2000 permutations, $p < .05$) for mean time-frequency topoplots at left frontal electrodes, nor in any other (**Figure 2**, second row).

Again, early, low-frequency modulations were present for Rejection-Compatible and Rejection-Incompatible conditions (2000 permutations, bootstrapping, FDR, $p < .05$) relative to baseline at left frontal electrodes. Frequency averages (1 - 15 Hz) showed significant differences (2000 permutations, bootstrapping, FDR, $p < .05$) between conditions throughout most of the Anticipatory phase. Contrastingly to HEP results, in this case, larger effects were associated with Rejection-Incompatible trials. In addition, mean time-frequency topoplots for the subtraction between conditions showed differences in frontal electrodes, particularly in left ones, as reflected by significantly clustered electrodes (2000 permutations, $p < .05$) (**Figure 2**, third row).

In summary, early activity in the frequency band of 1-15 Hz was present across conditions, presenting incremented ERSP during Acceptance (versus Rejection) and Incompatible-Rejection (versus Compatible-Rejection) trials at central- and left-frontal electrodes.

INSERT FIGURE 2 HERE

Figure 2. EEG results. *Left column*: Pre-feedback HEP. Grey-colored portions represent sustained (30 ms) significant differences between conditions (5000 permutations, FDR, $p < .05$), while obscured panels reflect non-significant results in the time window considered.

Topoplots illustrate the average subtraction of HEP between conditions in their respective significant difference time window. *Middle columns*: Time-frequency charts. Non-significant modulations (2000 permutations, bootstrapping, FDR, $p < .05$) relative to baseline were masked with value 1. Obscured panels reflect a non-significant difference between averages (right column). *Right column*: Average oscillations within the 1-15 HZ frequency range. Grey-colored portions indicate significant differences between conditions sustained at least over 150 ms (5000 permutations, bootstrapping, FDR, $p < .05$). Topoplots present the subtraction of average time-frequency (-2000 to 0 ms) between conditions. Black circles illustrate electrodes included in the calculation of the time-frequency charts, while magenta circles represent those included in significant frequency clusters (2000 permutations, cluster-based analysis, $p < .05$), and black circles with magenta borders were both included in the time-frequency chart analyses and presented significant differences in the cluster analysis. Obscured panels reflect non-significant findings (1-15 Hz). ERSP: event-related spectral perturbation.

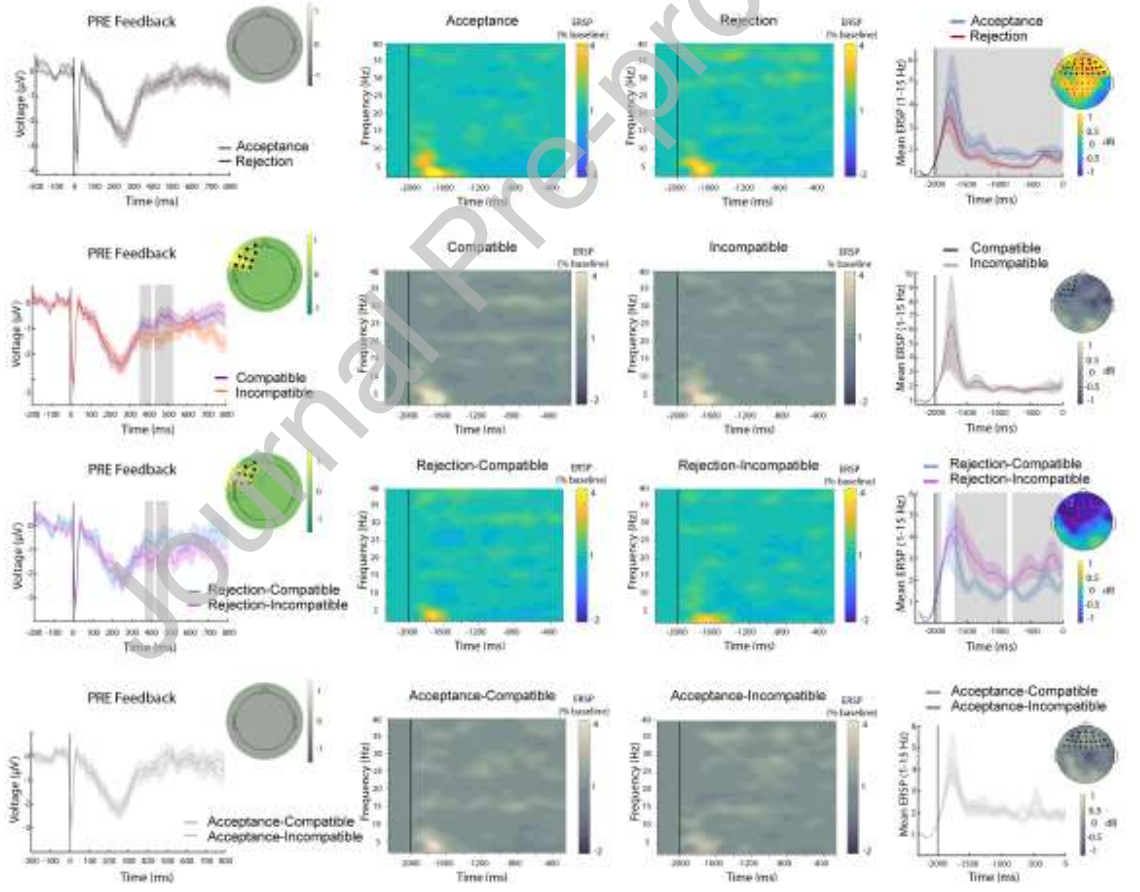

iEEG: Signals related to anticipation emerged from interoceptive hubs

To study anticipatory effects with a greater spatial and oscillatory resolution, iEEG recordings of two patients were analyzed (Subjects 2 and 3, **Figure 3**).

iHEP: Results were obtained by statistically comparing conditions of interest (5000 permutations, bootstrapping, FDR, $p < .05$) during the Anticipatory phase (after Guess through to Feedback). In the case of the contrast between Acceptance vs Rejection trials, larger effects for Acceptance in precentral and middle temporal areas were observed and no significant effects were found for Rejection trials. Comparison between Compatible and Incompatible trials revealed differences in frontal and limbic areas (superior frontal and anterior cingulate cortex), the insula, and parietal regions (inferior parietal and postcentral lobules). Within Rejection trials, Compatible vs Incompatible ones were discriminated in the left inferior frontal cortex, as well as frontal (right inferior frontal cortex), insula, and parietal regions (postcentral cortex). Acceptance trials presented a significant effect only for Compatible trials within the anterior cingulate cortex.

Time-frequency: Comparisons (5000 permutations, bootstrapping, FDR, $p < .05$) between conditions showed that Acceptance trials were associated with lower frequency ranges (delta, theta, alpha) mostly in frontal, limbic, and insular regions concerning Rejection trials that modulated higher frequencies (beta, gamma, hfo) in distributed brain regions (frontal, limbic, insular, parietal and temporal areas). As to Compatible vs Incompatible effects (5000 permutations, bootstrapping, FDR, $p < .05$), Compatible trials showed greater modulations at higher frequencies (beta, gamma, and hfo) mostly in temporal areas, while Incompatible trials at lower frequencies (delta, alpha, beta, gamma) in frontal, insular, and temporal regions. Noticeably, insular modulations were present for both conditions at different frequency bands (gamma for Compatible and alpha for Incompatible). Finally, both Acceptance (Compatible vs Incompatible) and Rejection (Compatible vs Incompatible) patterns were distributed from conditions in both spatial and frequency domains (2000 permutations, bootstrapping, FDR, $p < .05$).

In summary, iHEP results replicated those of HEP by showing that interoceptive signals were mostly modulated by uncertainty in key interoceptive hubs. Contrarily, intracranial exteroceptive signals were distributed across conditions, frequency bands, and cortex regions.

INSERT FIGURE 3 HERE

Figure 3. iEEG results. *Upper row*: Electrode localization. Subjects are color-coded. Black color represents contact sites that were discarded during preprocessing. *Middle row*: HEP results. Circular plots represent conditions (upper semi-circle) and contact sites that presented a significant heart-evoked potential (5000 permutations, FDR, $p < .05$) result in any condition sustained for at least 30 ms. *Bottom row*: Average oscillations for regions that presented significant differences (5000 permutations, bootstrapping, FDR, $p < .05$) between conditions in the same direction for at least 150 ms. Circular plots represent

frequency ranges (upper semi-circle) and brain regions with significant modulations in any frequency range (lower semi-circle). Links are color-coded according to the condition with larger modulation effects. HEP: heart-evoked potential; L: left; R: right; See **Table 1** for brain regions abbreviations.

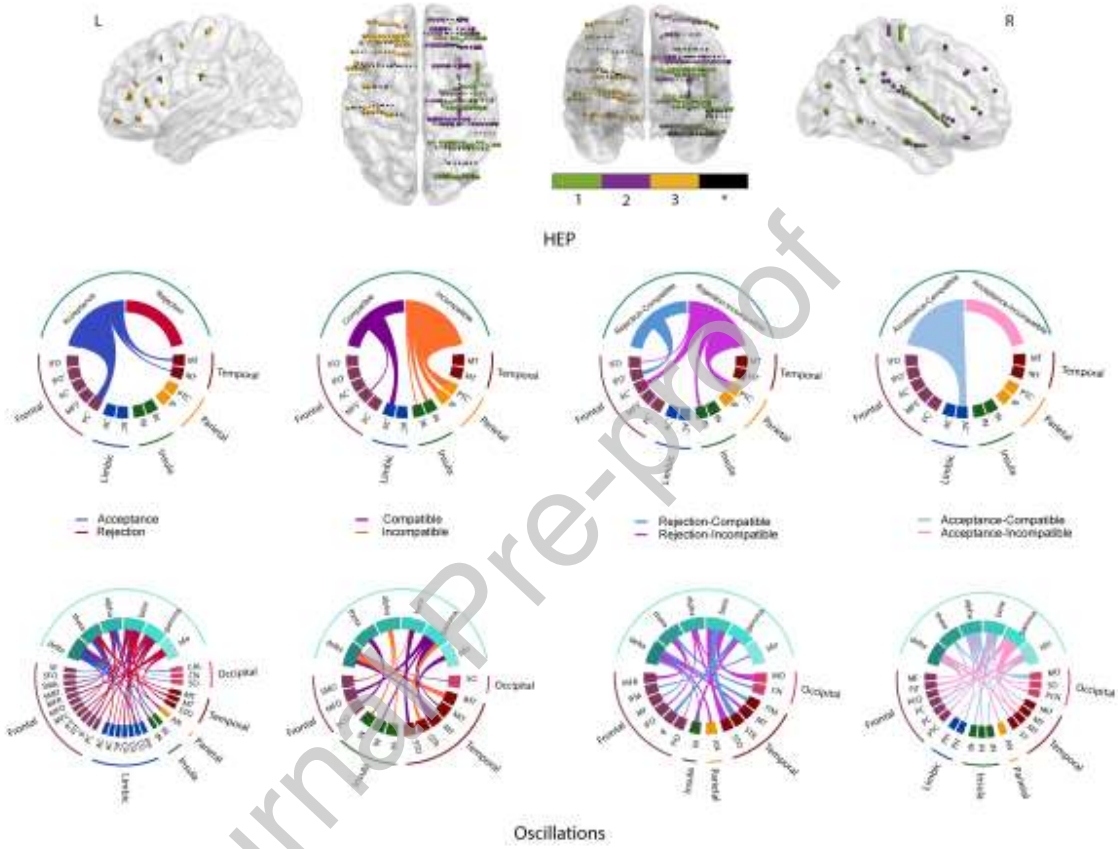

Table 1. Abbreviations used to reference brain regions in Figure 3.

Lobe	Abbreviation	Region
Frontal	SF	Superior frontal
	SFO	Superior frontal – orbital
	SMA	Superior motor area
	FSO	Frontal superior orbital
	MFS	Medial frontal – frontal superior
	MFC	Medial frontal – cingulum
	MFR	Medial frontal – rectus
	IFM	Inferior frontal – frontal mid
	MF	Middle frontal
	IF	Inferior frontal

	FIT	Inferior frontal - triangular
	IFO	Inferior frontal – orbital
	PC	Precentral
	PCO	Precentral – Rolandic operculum
	PTC	Postcentral
Limbic	AC	Anterior cingulate
	PH	Parahippocampal
Insula	IN	Insula
Parietal	MA	Supramarginal – angular
	IP	Inferior parietal lobule
Temporal	STR	Superior temporal – Rolandic operculum
	STO	Superior temporal – orbital
	MT	Middle temporal
	IT	Inferior temporal
Occipital	SO	Superior occipital
	MO	Middle occipital
	PCN	Precuneus
	CAL	Cuneus – calcarine
	CN	Cuneus

Summarizing, anticipatory interoceptive signals increased during Incompatible trials, reflected in larger negative HEP modulations. Also, within Rejection trials, Incompatible ones yielded larger negative HEP modulations than Compatible trials. These signals emerged from frontal and limbic areas, the insula, and parietal regions, as shown by intracranial recordings. Anticipatory exteroceptive signals were characterized by the presence of early activity between 1-15 Hz indiscriminately across conditions, with greater ERSP during Acceptance (versus Rejection) and Incompatible-Rejection (versus Compatible-Rejection) trials, observed over distributed conditions, frequency bands, and brain regions

Discussion

This study characterized anticipatory interoceptive and oscillatory brain activity during social rejection. The results are consistent with an allostatic-interoceptive predictive coding framework (Kleckner et al., 2017; Migeot et al., 2022; Nord and Garfinkel, 2022; Petzschner et al., 2021; Quigley et al., 2021; Schulkin and Sterling, 2019; Sterling, 2014),

posing that the brain regulates the body's internal milieu to prepare the organism for an eventual environmental challenge: a social rejection. As hypothesized, interoceptive signals were modulated by the level of uncertainty during the anticipation of the social outcome (unexpected social outcomes). Convergently, such signals emerged from key brain allostatic-interoceptive network hubs, as shown by iHEP modulations. On the other hand, exteroceptive signals were modulated by the anticipation of reward-related outcomes and observed over distributed regions. These findings may provide new insights for the study of the allostatic-interoceptive system and the development of more integrative social stress models.

Larger negative HEP modulations were present when the anticipation of feedback to the invite was uncertain. Enhancement of interoceptive processing has been observed during the anticipation of a social outcome (Durlik et al., 2014; Stevens et al., 2011; Wu et al., 2021), and our results expand those findings by informing the electrophysiological activity underlying the interoceptive processing under social uncertainty. Interestingly, when extending this result by exploring the interaction between Accepted/Rejected and Compatible/Incompatible conditions, the HEP modulation was larger when the feedback was Incompatible only during Rejection-guessed trials. This result is consistent with the findings of Durlik et al. (2014), who showed that interoceptive processing enhancement during anticipation of public speaking is positively correlated with fear of negative evaluations. Moreover, this finding could be interpreted under the negative expectancy bias effect (Cao et al., 2015; Gu et al., 2020; van der Molen et al., 2018), which describes a cognitive distortion characterized by the salience of the anticipation of negative outcomes during social interactions. Such cognitive distortion can be accompanied by a mismatch bias, which occurs when the positive evaluation of a peer evokes the anticipation of being negatively viewed by that peer (Smith et al., 2018). Arguably, sending the invite to a likable or popular peer would increase the salience of rejection, which would increase interoceptive processing. In summary, we showed that the enhancement of interoceptive processing is modulated by the uncertainty and valence of the social outcome, reflected in larger negative HEP modulations when guessing rejection and being uncertain about the social outcome. Our results further characterize interoceptive processing during the anticipation of a social outcome, which could be helpful to elucidate the inconsistent results in the field regarding the effect of social stress on interoceptive processing (Durlik et al., 2014; Stevens et al., 2011; Wu et al., 2021).

Early activity in the low-frequency band of 1-15 Hz was prominent across conditions. We replicated the previous involvement of low-frequency oscillatory activity during anticipation of social outcomes, linked with inhibitory control elicited by social stress (Hofmann, 2006; Hofmann et al., 2005; Vanhollebeke et al., 2022). Moreover, we found that the oscillatory activity was more prominent during Accepted vs. Rejected trials. This result is in line with evidence showing that oscillatory activity is systematically prominent when expecting a reward (e.g., acceptance of the invite) versus no reward (e.g., rejection of

the invite) (Alicart et al., 2015; Byrne et al., 2022; Fryer et al., 2021; Glazer et al., 2018; Gruber et al., 2013; Manssuer et al., 2022; Pornpattananangkul and Nusslock, 2016), explained by preparatory attentional relocation processes (Pornpattananangkul and Nusslock, 2016) and motivated-learning by feedback (Gruber et al., 2013). Further, when exploring the interaction between Accepted/Rejected and Compatible/Incompatible conditions, we found that Incompatible-Rejected trials displayed larger modulation. This result aligns with reward anticipation literature by interpreting Incompatible-Rejected trials as the anticipation of a near-miss event, described as situations where the probability of a negative outcome is very close to that of a favorable reward-related outcome (Alicart et al., 2015; Fryer et al., 2021). Then, Incompatible-Rejection, versus Compatible-Rejection trials, would increase the oscillations as the possibility of the acceptance of the invite is still motivationally present despite guessing rejection, versus resigning by anticipating the rejection. Convergently, low-frequency oscillatory activity is predominantly present during near-miss events (Alicart et al., 2015; Fryer et al., 2021). On the other hand, the difference between Incompatible vs. Compatible conditions would not be expected when guessing Acceptance, because the possibility of a favorable reward-related outcome (e.g., the acceptance of the invite) is anticipated in both scenarios. Thus, the occurrence of this outcome would be framed as probable rather than a near-miss event. In summary, our results contribute to the characterization of the oscillatory activity linked to the anticipation of a social outcome. Here, for the first time, we compared anticipatory oscillatory activity between different levels of uncertainty and valence, while most studies focus on the reactive and recovery phases, and evoked rather than oscillatory activity (Glazer et al., 2018; Meyer et al., 2021; Vanhollebeke et al., 2022).

Theoretical models and interpretations about interoceptive processing involved in the anticipation of a social outcome are controversial and often presented with inconsistent results. A novel allostatic-interoceptive predictive coding framework (Kleckner et al., 2017; Migeot et al., 2022; Nord and Garfinkel, 2022; Petzschner et al., 2021; Quigley et al., 2021; Schulkin and Sterling, 2019; Sterling, 2014) might illuminate the phenomenon. We found that social rejection consistently engaged regions of the allostatic-interoceptive network (Kleckner et al., 2017), corroborating previous HEP source localization studies (Birba et al., 2022; Legaz et al., 2020; Pollatos et al., 2005) by showing that HEP signals originated in key allostatic-interoceptive network hubs (as reflected by intracranial recordings), such as the anterior cingulate, insular, and prefrontal cortex. Contrarily, exteroceptive signals originated in distributed regions across the cerebral cortex, congruently with areas associated with reward processing, such as the frontal, centro-parietal, parieto-occipital, and temporal cortex regions (Glazer et al., 2018; Meyer et al., 2021). Thus, our results have relevant theoretical implications in further describing the allostatic-interoceptive process involved in the anticipation of a social outcome, characterized by a regulation of the body's internal milieu to prepare the organism for a social rejection.

Our study focuses on the anticipation of social rejection, bearing relevant implications to the development of the social stress framework. Theory-guided models of social stress can be extended with the allostatic interoceptive framework to study reactive and recovery phases and other forms of social stress (e.g., devaluating social comparison, hypervigilance of negative social cues). Also, our findings are aligned with and could potentially contribute to related emerging frameworks, such as the social allostasis model of loneliness (Mathew et al., 2020; Quadt et al., 2020; Saxbe et al., 2019) and the impact of social disparity on allostatic load (Ribeiro et al., 2018; Ribeiro et al., 2019). Future studies should incorporate relevant social stress measures, such as perceived social support (Bobba-Alves et al., 2022), and inter/intra-variability in stress resilience (Rao and Androulakis, 2019). Relatedly, considering the cross-cultural variability (Quesque et al., 2022) in social cognition domains (e.g., emotion recognition (Möller et al., 2022), theory of mind (Wang et al., 2022)), in social rejection sensitivity (Lou and Li, 2017; Sato et al., 2014), future studies should account for potential cultural differences in the perception of social rejection.

Some limitations and future directions of this work must be acknowledged. First, the age of the participants varied considerably, involving different stages of development. Indeed, interoceptive ability changes across the lifespan, for instance, decreasing during adolescence and being associated with brain maturational processes (Murphy et al., 2017). Nevertheless, contrary to related studies reporting similar age ranges (Smith et al., 2018), we employed age-appropriate faces from 8-10, 12-14, and 16-18 years old as stimuli, thus matching the age of the participant and the set of stimuli presented. Also, we assessed the potential confounding of age-effects in the HEP modulations and oscillatory activity. No significant impact of age was observed on the reported metrics (**Supplementary Material 3 and 4**). Second, although intracranial measures provide a unique approach compared to other non-invasive methods, they are only obtained from adult epileptic patients, who considerably differed in terms of age from the EEG sample and present caveats in terms of potential pathophysiological processes. Nevertheless, we have controlled this limitation by taking several cautious measures (Hesse, 2022): (i) we followed standard analysis protocols and performed a careful individual visual inspection of the iEEG channels, discarding those that presented pathological or artefactual waveforms, excessive power, and/or were placed in white matter or epileptogenic zones; (ii) we replicated the effects found in the EEG sample, even when the results could be confounded by brain maturational processes (Murphy et al., 2017); (iii) and guided our hypothesis and analysis from a non-invasive neuroimaging framework (Birba et al., 2022; Kleckner et al., 2017), thus suggesting that despite the limitations our conclusions are well-founded. Finally, we did not include behavioral and self-report measures assessing relevant factors during the anticipation of the social outcome, such as the level of uncertainty and its relationship with anxiety, thus precluding a direct assessment of the degree of uncertainty induced by the social rejection

task and the influence of confounding variables. Even though the employment of the HEP during noncardiac monitoring tasks has been systematically reported in the literature as a reliable and validated measure of interoceptive processing (Coll et al., 2021), suggestively associated with organismic processes to cope with uncertainty (Tumati et al., 2021), and recent meta-analytical evidence shows no evidence for an association between anxiety and interoceptive processing (Adams et al., 2022), future studies should implement behavioral designs (e.g., (Durlik et al., 2014; Durlik and Tsakiris, 2015; Stevens et al., 2011; Wu et al., 2021)) accompanied by self-report and EEG measures.

Conclusions

Our study suggests that the anticipation of a social outcome is characterized by allostatic-interoceptive processing focused on preparing the organism to face social rejection. Results provide a novel approach for the study of the allostatic-interoceptive system and to advance the development of more integrative social stress models, which may involve multiple levels of functioning to study normal and dysfunctional social behavior.

References

Adams, K.L., Edwards, A., Peart, C., Ellett, L., Mendes, I., Bird, G., Murphy, J., 2022. The association between anxiety and cardiac interoceptive accuracy: A systematic review and meta-analysis. Neuroscience & Biobehavioral Reviews 140, 104754. doi: 10.1016/j.neubiorev.2022.104754

Alicart, H., Cucurell, D., Mas-Herrero, E., Marco-Pallarés, J., 2015. Human oscillatory activity in near-miss events. Social cognitive and affective neuroscience 10, 1405-1412. doi: 10.1093/scan/nsv033

Ashburner, J., Friston, K., 1997. Multimodal image coregistration and partitioning--a unified framework. NeuroImage 6, 209-217. doi: 10.1006/nimg.1997.0290

Billeke, P., Armijo, A., Castillo, D., López, T., Zamorano, F., Cosmelli, D., Aboitiz, F., 2015. Paradoxical Expectation: Oscillatory Brain Activity Reveals Social Interaction Impairment in Schizophrenia. Biological Psychiatry 78, 421-431. doi: 10.1016/j.biopsych.2015.02.012

Billeke, P., Ossandon, T., Perrone-Bertolotti, M., Kahane, P., Bastin, J., Jerbi, K., Lachaux, J.-P., Fuentealba, P., 2020. Human Anterior Insula Encodes Performance Feedback and Relays Prediction Error to the Medial Prefrontal Cortex. Cerebral Cortex 30, 4011-4025. doi: 10.1093/cercor/bhaa017

Billeke, P., Zamorano, F., López, T., Rodriguez, C., Cosmelli, D., Aboitiz, F., 2014. Someone has to give in: theta oscillations correlate with adaptive behavior in social bargaining. Social cognitive and affective neuroscience 9, 2041-2048. doi: 10.1093/scan/nsu012

Birba, A., Hesse, E., Sedeno, L., Mikulan, E.P., Garcia, M.D.C., Avalos, J., Adolfi, F., Legaz, A., Bekinschtein, T.A., Zimerman, M., Parra, M., Garcia, A.M., Ibanez, A., 2017. Enhanced Working Memory Binding by Direct Electrical Stimulation of the Parietal Cortex. Frontiers in Aging Neuroscience 9, 178. doi: 10.3389/fnagi.2017.00178

Birba, A., Santamaria-Garcia, H., Prado, P., Cruzat, J., Ballesteros, A.S., Legaz, A., Fittipaldi, S., Duran-Aniotz, C., Slachevsky, A., Santibanez, R., Sigman, M., Garcia, A.M., Whelan, R., Moguilner, S., Ibanez, A., 2022. Allostatic-Interoceptive Overload in Frontotemporal Dementia. Biological Psychiatry. doi: 10.1016/j.biopsych.2022.02.955

Blakemore, S.J., Mills, K.L., 2014. Is adolescence a sensitive period for sociocultural processing? Annual Review of Psychology 65, 187-207. doi: 10.1146/annurev-psych-010213-115202

Bobba-Alves, N., Juster, R.-P., Picard, M., 2022. The energetic cost of allostasis and allostatic load. Psychoneuroendocrinology 146, 105951. doi: 10.1016/j.psyneuen.2022.105951

Byrne, A., Hewitt, D., Henderson, J., Newton-Fenner, A., Roberts, H., Tyson-Carr, J., Fallon, N., Giesbrecht, T., Stancak, A., 2022. Investigating the effect of losses and gains on effortful engagement during an incentivized Go/NoGo task through anticipatory cortical oscillatory changes. Psychophysiology 59, e13897. doi: 10.1111/psyp.13897

Cao, J., Gu, R., Bi, X., Zhu, X., Wu, H., 2015. Unexpected Acceptance? Patients with Social Anxiety Disorder Manifest their Social Expectancy in ERPs During Social Feedback Processing. Frontiers in Psychology 6. doi: 10.3389/fpsyg.2015.01745

Chae, Y., Park, H.-J., Lee, I.-S., 2022. Pain modalities in the body and brain: Current knowledge and future perspectives. Neuroscience & Biobehavioral Reviews 139, 104744. doi: 10.1016/j.neubiorev.2022.104744

Chennu, S., Noreika, V., Gueorguiev, D., Blenkmann, A., Kochen, S., Ibáñez, A., Owen, A.M., Bekinschtein, T.A., 2013. Expectation and attention in hierarchical auditory prediction. Journal of Neuroscience 33, 11194-11205. doi: 10.1523/jneurosci.0114-13.2013

Coll, M.P., Hobson, H., Bird, G., Murphy, J., 2021. Systematic review and meta-analysis of the relationship between the heartbeat-evoked potential and interoception. Neuroscience & Biobehavioral Reviews 122, 190-200. doi: 10.1016/j.neubiorev.2020.12.012

Couto, B., Adolfi, F., Velasquez, M., Mesow, M., Feinstein, J., Canales-Johnson, A., Mikulan, E., Martinez-Pernia, D., Bekinschtein, T., Sigman, M., Manes, F., Ibanez, A., 2015. Heart evoked potential triggers brain responses to natural affective scenes: A preliminary study. Autonomic Neuroscience 193, 132-137. doi:

Couto, B., Salles, A., Sedeno, L., Peradejordi, M., Barttfeld, P., Canales-Johnson, A., Dos Santos, Y.V., Huepe, D., Bekinschtein, T., Sigman, M., Favaloro, R., Manes, F., Ibanez, A., 2014. The man who feels two hearts: the different pathways of interoception. Social Cognitive and Affective Neuroscience 9, 1253-1260. doi: 10.1093/scan/nst108

Delorme, A., Makeig, S., 2004. EEGLAB: an open source toolbox for analysis of single-trial EEG dynamics including independent component analysis. Journal of Neuroscience Methods 134, 9-21. doi: 10.1016/j.jneumeth.2003.10.009

Durlik, C., Brown, G., Tsakiris, M., 2014. Enhanced interoceptive awareness during anticipation of public speaking is associated with fear of negative evaluation. Cognition and Emotion 28, 530-540. doi: 10.1080/02699931.2013.832654
Durlik, C., Tsakiris, M., 2015. Decreased interoceptive accuracy following social exclusion. International Journal of Psychophysiology 96, 57-63. doi: 10.1016/j.ijpsycho.2015.02.020
Eisenberger, N.I., 2012. The pain of social disconnection: examining the shared neural underpinnings of physical and social pain. Nature Reviews Neuroscience 13, 421-434. doi: 10.1038/nrn3231
Eisenberger, N.I., 2015. Social Pain and the Brain: Controversies, Questions, and Where to Go from Here. Annual Review of Psychology 66, 601-629. doi: 10.1146/annurev-psych-010213-115146
Foster, B.L., Rangarajan, V., Shirer, W.R., Parvizi, J., 2015. Intrinsic and task-dependent coupling of neuronal population activity in human parietal cortex. Neuron 86, 578-590. doi: 10.1016/j.neuron.2015.03.018
Fryer, S.L., Roach, B.J., Holroyd, C.B., Paulus, M.P., Sargent, K., Boos, A., Ford, J.M., Mathalon, D.H., 2021. Electrophysiological investigation of reward anticipation and outcome evaluation during slot machine play. NeuroImage 232, 117874. doi: 10.1016/j.neuroimage.2021.117874
Garcia-Cordero, I., Esteves, S., Mikulan, E.P., Hesse, E., Baglivo, F.H., Silva, W., Garcia, M.D.C., Vaucheret, E., Ciraolo, C., Garcia, H.S., Adolfi, F., Pietto, M., Herrera, E., Legaz, A., Manes, F., Garcia, A.M., Sigman, M., Bekinschtein, T.A., Ibanez, A., Sedeno, L., 2017. Attention, in and Out: Scalp-Level and Intracranial EEG Correlates of Interoception and Exteroception. Frontiers in Neuroscience 11, 411. doi: 10.3389/fnins.2017.00411
Garcia-Cordero, I., Sedeno, L., de la Fuente, L., Slachevsky, A., Forno, G., Klein, F., Lillo, P., Ferrari, J., Rodriguez, C., Bustin, J., Torralva, T., Baez, S., Yoris, A., Esteves, S., Melloni, M., Salamone, P., Huepe, D., Manes, F., Garcia, A.M., Ibanez, A., 2016. Feeling, learning from and being aware of inner states: interoceptive dimensions in neurodegeneration and stroke. Philosophical Transactions of the Royal Society B: Biological Sciences 371. doi: 10.1098/rstb.2016.0006
Garcia, A.M., Hesse, E., Birba, A., Adolfi, F., Mikulan, E., Caro, M.M., Petroni, A., Bekinschtein, T.A., Del Carmen Garcia, M., Silva, W., Ciraolo, C., Vaucheret, E., Sedeno, L., Ibanez, A., 2020. Time to Face Language: Embodied Mechanisms Underpin the Inception of Face-Related Meanings in the Human Brain. Cerebral Cortex. doi: 10.1093/cercor/bhaa178
Glazer, J.E., Kelley, N.J., Pornpattananangkul, N., Mittal, V.A., Nusslock, R., 2018. Beyond the FRN: Broadening the time-course of EEG and ERP components implicated in reward processing. International Journal of Psychophysiology 132, 184-202. doi: 10.1016/j.ijpsycho.2018.02.002

Gruber, M.J., Watrous, A.J., Ekstrom, A.D., Ranganath, C., Otten, L.J., 2013. Expected reward modulates encoding-related theta activity before an event. NeuroImage 64, 68-74. doi: 10.1016/j.neuroimage.2012.07.064

Gu, R., Ao, X., Mo, L., Zhang, D., 2020. Neural correlates of negative expectancy and impaired social feedback processing in social anxiety. Social cognitive and affective neuroscience 15, 285-291. doi: 10.1093/scan/nsaa038

Gu, Z., Gu, L., Eils, R., Schlesner, M., Brors, B., 2014. circlize Implements and enhances circular visualization in R. Bioinformatics 30, 2811-2812. doi: 10.1093/bioinformatics/btu393

Hesse, E., 2022. Intracranial Studies of Cognition in Humans. In: Della Sala, S. (Ed.), Encyclopedia of Behavioral Neuroscience, 2nd edition (Second Edition). Elsevier, Oxford, pp. 203-219.

Hesse, E., Mikulan, E., Decety, J., Sigman, M., Garcia, M.d.C., Silva, W., Ciraolo, C., Vaucheret, E., Baglivo, F., Huepe, D., Lopez, V., Manes, F., Bekinschtein, T.A., Ibanez, A., 2016a. Early detection of intentional harm in the human amygdala. Brain 139, 54-61. doi: 10.1093/brain/awv336

Hesse, E., Mikulan, E., Decety, J., Sigman, M., Garcia Mdel, C., Silva, W., Ciraolo, C., Vaucheret, E., Baglivo, F., Huepe, D., Lopez, V., Manes, F., Bekinschtein, T.A., Ibanez, A., 2016b. Early detection of intentional harm in the human amygdala. Brain 139, 54-61. doi: 10.1093/brain/awv336

Hesse, E., Mikulan, E., Sitt, J.D., Garcia, M.D.C., Silva, W., Ciraolo, C., Vaucheret, E., Raimondo, F., Baglivo, F., Adolfi, F., Herrera, E., Bekinschtein, T.A., Petroni, A., Lew, S., Sedeno, L., Garcia, A.M., Ibanez, A., 2019. Consistent gradient of performance and decoding of stimulus type and valence from local and network activity. IEEE Transactions on Neural Systems and Rehabilitation Engineering. doi: 10.1109/TNSRE.2019.2903921

Higham, D., Higham, N., 2016. MATLAB guide. Siam.

Hofmann, S.G., 2006. The emotional consequences of social pragmatism: The psychophysiological correlates of self-monitoring. Biological Psychology 73, 169-174. doi: 10.1016/j.biopsycho.2006.03.001

Hofmann, S.G., Moscovitch, D.A., Litz, B.T., Kim, H.J., Davis, L.L., Pizzagalli, D.A., 2005. The worried mind: autonomic and prefrontal activation during worrying. Emotion 5, 464-475. doi: 10.1037/1528-3542.5.4.464

Kern, M., Aertsen, A., Schulze-Bonhage, A., Ball, T., 2013. Heart cycle-related effects on event-related potentials, spectral power changes, and connectivity patterns in the human ECoG. NeuroImage 81, 178-190. doi: 10.1016/j.neuroimage.2013.05.042

Kim, D., Kim, S.K., 2012. Comparing patterns of component loadings: principal component analysis (PCA) versus independent component analysis (ICA) in analyzing multivariate non-normal data. Behavior Research Methods 44, 1239-1243. doi: 10.3758/s13428-012-0193-1

Kleckner, I.R., Zhang, J., Touroutoglou, A., Chanes, L., Xia, C., Simmons, W.K., Quigley, K.S., Dickerson, B.C., Feldman Barrett, L., 2017. Evidence for a large-scale brain system

supporting allostasis and interoception in humans. Nature Human Behaviour 1. doi: 10.1038/s41562-017-0069
Laceulle, O.M., Veenstra, R., Vollebergh, W.A.M., Ormel, J., 2019. Sequences of maladaptation: Preadolescent self-regulation, adolescent negative social interactions, and young adult psychopathology. Development and Psychopathology 31, 279-292. doi: 10.1017/S0954579417001808
Larrabee Sonderlund, A., Thilsing, T., Sondergaard, J., 2019. Should social disconnectedness be included in primary-care screening for cardiometabolic disease? A systematic review of the relationship between everyday stress, social connectedness, and allostatic load. PLoS One 14, e0226717. doi: 10.1371/journal.pone.0226717
Legaz, A., Yoris, A., Sedeño, L., Abrevaya, S., Martorell, M., Alifano, F., García, A.M., Ibañez, A., 2020. Heart–brain interactions during social and cognitive stress in hypertensive disease: A multidimensional approach. European Journal of Neuroscience. doi: 10.1111/ejn.14979
Legaz, A., Yoris, A., Sedeño, L., Abrevaya, S., Martorell, M., Alifano, F., García, A.M., Ibañez, A., 2022. Heart-brain interactions during social and cognitive stress in hypertensive disease: A multidimensional approach. European Journal of Neuroscience 55, 2836-2850. doi: 10.1111/ejn.14979
Lou, N.M., Li, L.M.W., 2017. Interpersonal relationship mindsets and rejection sensitivity across cultures: The role of relational mobility. Personality and Individual Differences 108, 200-206. doi: 10.1016/j.paid.2016.12.004
Manssuer, L., Wang, L., Ding, Q., Li, J., Zhang, Y., Zhang, C., Hallett, M., Li, D., Sun, B., Voon, V., 2022. Subthalamic Oscillatory Activity of Reward and Loss Processing Using the Monetary Incentive Delay Task in Parkinson Disease. Neuromodulation: Technology at the Neural Interface. doi: 10.1016/j.neurom.2022.04.033
Mathew, A., Doorenbos, A.Z., Li, H., Jang, M.K., Park, C.G., Bronas, U.G., 2020. Allostatic Load in Cancer: A Systematic Review and Mini Meta-Analysis. Biological Research For Nursing 23, 341-361. doi: 10.1177/1099800420969898
Meyer, G.M., Marco-Pallarés, J., Boulinguez, P., Sescousse, G., 2021. Electrophysiological underpinnings of reward processing: Are we exploiting the full potential of EEG? NeuroImage 242, 118478. doi: 10.1016/j.neuroimage.2021.118478
Migeot, J., Duran-Aniotz, C., Signorelli, C.M., Piguet, O., Ibáñez, A., 2022. A predictive coding framework of allostatic-interoceptive overload in frontotemporal dementia. Trends in Neurosciences 45, 838-853. doi: 10.1016/j.tins.2022.08.005
Mikulan, E., Hesse, E., Sedeno, L., Bekinschtein, T., Sigman, M., Garcia, M.D.C., Silva, W., Ciraolo, C., Garcia, A.M., Ibanez, A., 2018a. Intracranial high-gamma connectivity distinguishes wakefulness from sleep. NeuroImage 169, 265-277. doi: 10.1016/j.neuroimage.2017.12.015
Mikulan, E., Hesse, E., Sedeño, L., Bekinschtein, T., Sigman, M., García, M.d.C., Silva, W., Ciraolo, C., García, A.M., Ibáñez, A., 2018b. Intracranial high-γ connectivity

distinguishes wakefulness from sleep. NeuroImage 169, 265-277. doi: 10.1016/j.neuroimage.2017.12.015
Möller, C., Bull, R., Aschersleben, G., 2022. Culture shapes preschoolers' emotion recognition but not emotion comprehension: a cross-cultural study in Germany and Singapore. Journal of Cultural Cognitive Science 6, 9-25. doi: 10.1007/s41809-021-00093-6
Muller, L.E., Schulz, A., Andermann, M., Gabel, A., Gescher, D.M., Spohn, A., Herpertz, S.C., Bertsch, K., 2015. Cortical Representation of Afferent Bodily Signals in Borderline Personality Disorder: Neural Correlates and Relationship to Emotional Dysregulation. JAMA Psychiatry 72, 1077-1086. doi: 10.1001/jamapsychiatry.2015.1252
Murphy, J., Brewer, R., Catmur, C., Bird, G., 2017. Interoception and psychopathology: A developmental neuroscience perspective. Developmental Cognitive Neuroscience 23, 45-56. doi: 10.1016/j.dcn.2016.12.006
Nord, C.L., Garfinkel, S.N., 2022. Interoceptive pathways to understand and treat mental health conditions. Trends in Cognitive Sciences doi: 10.1016/j.tics.2022.03.004
Oostenveld, R., Fries, P., Maris, E., Schoffelen, J.M., 2011. FieldTrip: Open source software for advanced analysis of MEG, EEG, and invasive electrophysiological data. Computational Intelligence and Neuroscience 2011, 156869. doi: 10.1155/2011/156869
Orben, A., Tomova, L., Blakemore, S.J., 2020. The effects of social deprivation on adolescent development and mental health. The Lancet Child & Adolescent Health 4, 634-640. doi: 10.1016/s2352-4642(20)30186-3
Park, H.D., Bernasconi, F., Salomon, R., Tallon-Baudry, C., Spinelli, L., Seeck, M., Schaller, K., Blanke, O., 2018. Neural Sources and Underlying Mechanisms of Neural Responses to Heartbeats, and their Role in Bodily Self-consciousness: An Intracranial EEG Study. Cerebral Cortex 28, 2351-2364. doi: 10.1093/cercor/bhx136
Park, H.D., Correia, S., Ducorps, A., Tallon-Baudry, C., 2014. Spontaneous fluctuations in neural responses to heartbeats predict visual detection. Nature Neuroscience 17, 612-618. doi: 10.1038/nn.3671
Parvizi, J., Kastner, S., 2018. Promises and limitations of human intracranial electroencephalography. Nat Neurosci 21, 474-483. doi: 10.1038/s41593-018-0108-2
Peters, A., McEwen, B.S., Friston, K., 2017. Uncertainty and stress: Why it causes diseases and how it is mastered by the brain. Progress in Neurobiology 156, 164-188. doi: 10.1016/j.pneurobio.2017.05.004
Petzschner, F.H., Garfinkel, S.N., Paulus, M.P., Koch, C., Khalsa, S.S., 2021. Computational Models of Interoception and Body Regulation. Trends in Neurosciences 44, 63-76. doi: 10.1016/j.tins.2020.09.012
Pollatos, O., Herbert, B.M., Mai, S., Kammer, T., 2016. Changes in interoceptive processes following brain stimulation. Philosophical Transactions of the Royal Society B: Biological Sciences 371. doi: 10.1098/rstb.2016.0016

Pollatos, O., Kirsch, W., Schandry, R., 2005. Brain structures involved in interoceptive awareness and cardioafferent signal processing: a dipole source localization study. Human Brain Mapping 26, 54-64. doi: 10.1002/hbm.20121
Pollatos, O., Schandry, R., 2004. Accuracy of heartbeat perception is reflected in the amplitude of the heartbeat-evoked brain potential. Psychophysiology 41, 476-482. doi: 10.1111/1469-8986.2004.00170.x
Poppelaars, E.S., Harrewijn, A., Westenberg, P.M., van der Molen, M.J.W., 2018. Frontal delta-beta cross-frequency coupling in high and low social anxiety: An index of stress regulation? Cogn Affect Behav Neurosci 18, 764-777. doi: 10.3758/s13415-018-0603-7
Poppelaars, E.S., Klackl, J., Pletzer, B., Jonas, E., 2021. Delta-beta cross-frequency coupling as an index of stress regulation during social-evaluative threat. Biological Psychology 160, 108043. doi: 10.1016/j.biopsycho.2021.108043
Pornpattananangkul, N., Nusslock, R., 2016. Willing to wait: Elevated reward-processing EEG activity associated with a greater preference for larger-but-delayed rewards. Neuropsychologia 91, 141-162. doi: 10.1016/j.neuropsychologia.2016.07.037
Quadt, L., Esposito, G., Critchley, H.D., Garfinkel, S.N., 2020. Brain-body interactions underlying the association of loneliness with mental and physical health. Neuroscience & Biobehavioral Reviews 116, 283-300. doi: 10.1016/j.neubiorev.2020.06.015
Quesque, F., Coutrot, A., Cox, S., de Souza, L.C., Baez, S., Cardona, J.F., Mulet-Perreault, H., Flanagan, E., Neely-Prado, A., Clarens, M.F., Cassimiro, L., Musa, G., Kemp, J., Botzung, A., Philippi, N., Cosseddu, M., Trujillo-Llano, C., Grisales-Cardenas, J.S., Fittipaldi, S., Magrath Guimet, N., Calandri, I.L., Crivelli, L., Sedeno, L., Garcia, A.M., Moreno, F., Indakoetxea, B., Benussi, A., Brandão Moura, M.V., Santamaria-Garcia, H., Matallana, D., Pryanishnikova, G., Morozova, A., Iakovleva, O., Veryugina, N., Levin, O., Zhao, L., Liang, J., Duning, T., Lebouvier, T., Pasquier, F., Huepe, D., Barandiaran, M., Johnen, A., Lyashenko, E., Allegri, R.F., Borroni, B., Blanc, F., Wang, F., Yassuda, M.S., Lillo, P., Teixeira, A.L., Caramelli, P., Hudon, C., Slachevsky, A., Ibáñez, A., Hornberger, M., Bertoux, M., 2022. Does culture shape our understanding of others' thoughts and emotions? An investigation across 12 countries. Neuropsychology 36, 664-682. doi: 10.1037/neu0000817
Quigley, K.S., Kanoski, S., Grill, W.M., Barrett, L.F., Tsakiris, M., 2021. Functions of Interoception: From Energy Regulation to Experience of the Self. Trends in Neurosciences 44, 29-38. doi: 10.1016/j.tins.2020.09.008
Rao, R., Androulakis, I.P., 2019. The physiological significance of the circadian dynamics of the HPA axis: Interplay between circadian rhythms, allostasis and stress resilience. Hormones and Behavior 110, 77-89. doi: 10.1016/j.yhbeh.2019.02.018
Rappaport, B.I., Barch, D.M., 2020. Brain responses to social feedback in internalizing disorders: A comprehensive review. Neuroscience & Biobehavioral Reviews 118, 784-808. doi: 10.1016/j.neubiorev.2020.09.012
Raufelder, D., Neumann, N., Domin, M., Lorenz, R.C., Gleich, T., Golde, S., Romund, L., Beck, A., Hoferichter, F., 2021. Do Belonging and Social Exclusion at School Affect

Structural Brain Development During Adolescence? Child Development 92, 2213-2223. doi: 10.1111/cdev.13613
Ribeiro, A.I., Amaro, J., Lisi, C., Fraga, S., 2018. Neighborhood Socioeconomic Deprivation and Allostatic Load: A Scoping Review. International Journal of Environmental Research and Public Health 15. doi: 10.3390/ijerph15061092
Ribeiro, A.I., Fraga, S., Kelly-Irving, M., Delpierre, C., Stringhini, S., Kivimaki, M., Joost, S., Guessous, I., Gandini, M., Vineis, P., Barros, H., 2019. Neighbourhood socioeconomic deprivation and allostatic load: a multi-cohort study. Scientific Reports 9, 8790. doi: 10.1038/s41598-019-45432-4
Rorden, C., Brett, M., 2000. Stereotaxic display of brain lesions. Behavioural Neurology 12, 191-200. doi: 10.1155/2000/421719
Rosenblad, A. B. F. J., 2009. Manly: Randomization, bootstrap and Monte Carlo methods in biology, third edition. Computational Statistics 24, 371–372. doi: 10.1007/s00180-009-0150-3
Salamone, P.C., Sedeno, L., Legaz, A., Bekinschtein, T., Martorell, M., Adolfi, F., Fraile-Vazquez, M., Rodriguez Arriagada, N., Favaloro, L., Peradejordi, M., Absi, D.O., Garcia, A.M., Favaloro, R., Ibanez, A., 2020. Dynamic neurocognitive changes in interoception after heart transplant. Brain Communications 2, fcaa095. doi: 10.1093/braincomms/fcaa095
Sato, K., Yuki, M., Norasakkunkit, V., 2014. A Socio-Ecological Approach to Cross-Cultural Differences in the Sensitivity to Social Rejection: The Partially Mediating Role of Relational Mobility. Journal of Cross-Cultural Psychology 45, 1549-1560. doi: 10.1177/0022022114544320
Saxbe, D.E., Beckes, L., Stoycos, S.A., Coan, J.A., 2019. Social Allostasis and Social Allostatic Load: A New Model for Research in Social Dynamics, Stress, and Health. Perspectives on Psychological Science 15, 469-482. doi: 10.1177/1745691619876528
Schulkin, J., Sterling, P., 2019. Allostasis: A Brain-Centered, Predictive Mode of Physiological Regulation. Trends in Neurosciences 42, 740-752. doi: 10.1016/j.tins.2019.07.010
Smith, A.R., Nelson, E.E., Rappaport, B.I., Pine, D.S., Leibenluft, E., Jarcho, J.M., 2018. I Like Them… Will They Like Me? Evidence for the Role of the Ventrolateral Prefrontal Cortex During Mismatched Social Appraisals in Anxious Youth. Journal of Child and Adolescent Psychopharmacology 28, 646-654. doi: 10.1089/cap.2017.0142
Somerville, L.H., Heatherton, T.F., Kelley, W.M., 2006. Anterior cingulate cortex responds differentially to expectancy violation and social rejection. Nature Neuroscience 9, 1007-1008. doi: 10.1038/nn1728
Sterling, P., 2014. Homeostasis vs allostasis implications for brain function and mental disorders. JAMA Psychiatry 71, 1192-1193. doi: 10.1001/jamapsychiatry.2014.1043
Stevens, S., Gerlach, A.L., Cludius, B., Silkens, A., Craske, M.G., Hermann, C., 2011. Heartbeat perception in social anxiety before and during speech anticipation. Behaviour Research and Therapy 49, 138-143. doi: 10.1016/j.brat.2010.11.009

Stolk, A., Griffin, S., van der Meij, R., Dewar, C., Saez, I., Lin, J.J., Piantoni, G., Schoffelen, J.M., Knight, R.T., Oostenveld, R., 2018. Integrated analysis of anatomical and electrophysiological human intracranial data. Nature Protocols 13, 1699-1723. doi: 10.1038/s41596-018-0009-6

R Core Team, 2021. R: A anguage and Environment for Statistical Computing. R Foundation for Statistical Computing.

Tsakiris, M., Critchley, H., 2016. Interoception beyond homeostasis: affect, cognition and mental health. Philosophical Transactions of the Royal Society B: Biological Sciences 371, 20160002. doi: 10.1098/rstb.2016.0002

Tumati, S., Paulus, M.P., Northoff, G., 2021. Out-of-step: brain-heart desynchronization in anxiety disorders. Molecular Psychiatry 26, 1726-1737. doi: 10.1038/s41380-021-01029-w

Tyborowska, A., Volman, I., Niermann, H.C.M., Pouwels, J.L., Smeekens, S., Cillessen, A.H.N., Toni, I., Roelofs, K., 2018. Early-life and pubertal stress differentially modulate grey matter development in human adolescents. Scientific Reports 8, 9201. doi: 10.1038/s41598-018-27439-5

van der Molen, M.J.W., Harrewijn, A., Westenberg, P.M., 2018. Will they like me? Neural and behavioral responses to social-evaluative peer feedback in socially and non-socially anxious females. Biological Psychology 135, 18-28. doi: 10.1016/j.biopsycho.2018.02.016

Vanhollebeke, G., De Smet, S., De Raedt, R., Baeken, C., van Mierlo, P., Vanderhasselt, M.-A., 2022. The neural correlates of psychosocial stress: A systematic review and meta-analysis of spectral analysis EEG studies. Neurobiology of Stress 18, 100452. doi: 10.1016/j.ynstr.2022.100452

Wang, S., Andrews, G., Pendergast, D., Neumann, D., Chen, Y., Shum, D.H.K., 2022. A Cross-Cultural Study of Theory of Mind Using Strange Stories in School-Aged Children from Australia and Mainland China. Journal of Cognition and Development 23, 40-63. doi: 10.1080/15248372.2021.1974445

Wu, J., Li, H., Wu, Y., 2021. Trait and State: Interoceptive Accuracy during Anticipation of Public Speaking in Junior Secondary Shy Students from an Eastern Province of China. International Journal of Environmental Research and Public Health 18. doi: 10.3390/ijerph18094951

Xia, M., Wang, J., He, Y., 2013. BrainNet Viewer: a network visualization tool for human brain connectomics. PLoS One 8, e68910. doi: 10.1371/journal.pone.0068910

Yoris, A., Abrevaya, S., Esteves, S., Salamone, P., Lori, N., Martorell, M., Legaz, A., Alifano, F., Petroni, A., Sanchez, R., Sedeno, L., Garcia, A.M., Ibanez, A., 2018. Multilevel convergence of interoceptive impairments in hypertension: New evidence of disrupted body-brain interactions. Human Brain Mapping 39, 1563-1581. doi: 10.1002/hbm.23933

Yoris, A., Garcia, A.M., Traiber, L., Santamaria-Garcia, H., Martorell, M., Alifano, F., Kichic, R., Moser, J.S., Cetkovich, M., Manes, F., Ibanez, A., Sedeno, L., 2017. The inner world of overactive monitoring: neural markers of interoception in obsessive-compulsive disorder. Psychological Medicine 47, 1957-1970. doi: 10.1017/S0033291717000368

Data and code availability statements

Metadata will be made available to at Open Science Framework (OSF). A full (Raw) data request needs approval from the local ethics committee. All codes used in the study will be made available at OSF.

CAS
Joaquín Migeot: Writing - Original Draft; **Eugenia Hesse**: Methodology, Formal analysis, Data Curation, Writing - Original Draft, Visualization; **Sol Fittipaldi**: Writing - Review & Editing; **Jhonny Mejía**: Formal analysis, Data Curation; **Matías Fraile**: Formal analysis, Data Curation; **Adolfo M. García**: Review & Editing, **María del Carmen García**: Resources, **Rodrigo Ortega**: Review & Editing; **Brian Lawlor**: Review & Editing; **Vladimir Lopez**: Conceptualization, Methodology, Resources, Writing - Review & Editing, Supervision, Project administration, Funding acquisition; **Agustín Ibáñez**: Conceptualization, Methodology, Resources, Writing - Review & Editing, Supervision

Declaration of Interest Statement

None